

Removal of methylene blue from simulated wastewater by *Carica papaya* wood biosorbent

Thi Nhu Ngoc Nguyen*, Thi Thanh Hang Huynh, Thi Hien To

Faculty of Environment, University of Science, Vietnam National University, Ho Chi Minh city

Received 4 September 2020; accepted 3 December 2020

Abstract:

In this study, batch and continuous-flow sorption experiments were conducted to evaluate the removal of methylene blue (MB) from aqueous solutions by *Carica papaya* wood (CPW) biosorbents. The effects of critical factors such as initial pH, particle size of the biosorbent, biosorbent dosage, initial dye concentration, contact time, and salt ionic strength were studied in batch experiments. The equilibrium data fit well to the Langmuir isotherm model with the highest monolayer adsorption capacity of 63.29 mg/g at an initial dye concentration of 50 mg/l, pH of 10, and contact time of 60 min. Batch desorption and regeneration studies using 0.1 M HCl as the desorbing agent indicated that the removal efficiency of MB lasted up to 5 cycles. Continuous-flow biosorption experiments were investigated to determine the practical applicability of the biosorbent. The dye removal efficiency increased with an increase in adsorbent dosage and decreased with an increase in flow rate. The Thomas model was found to be in good agreement with all the experimental data collected from continuous flow sorption. It was concluded that this study presented CPW as a promising biosorbent material for the removal MB from aqueous solutions.

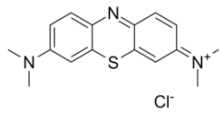
Keywords: biosorption, *Carica papaya* wood, desorption, methylene blue.

Classification number: 5.1

Introduction

Dye application occurs in several industries such as the textile, paper and pulp, paint, printing, rubber, and cosmetics industries. During the dyeing process, 1-15% of the dye is lost in the effluent discharge that generates endless quantities of dye-containing wastewater [1]. Synthetic dyes, characterized by complex aromatic structures, are stable enough to withstand heat and light and are considered non-biodegradable [2, 3]. Discharge of these dyes into effluent may impart toxicity to aquatic life and may be carcinogenic or mutagenic to human beings, which causes serious damage such as dysfunction of the kidneys, reproductive system, liver, brain, and central nervous system [4-6]. Methylene blue (MB) is a cationic dye that is widely used in dyeing cotton, wool, coloured paper, and coatings for paper stocks [7]. Table 1 represents the general characteristics of methylene blue.

Table 1. General characteristics of methylene blue.

Particulars	Methylene blue
Molecular structure	
Chemical formula	C ₁₆ H ₁₈ N ₃ SCl
Formula weight (g/mol)	319.85
Class	Cationic thiazine dye
Colour Index number	52015
Colour Index name	Basic Blue 9 (BG 9)
λ_{max} (nm)	664

Among the various techniques of dye removal, adsorption is a preferred procedure that demonstrates good performance as it can be used to remove different types of colour from materials [8-10]. Adsorption has been considered a superior method for water treatment in terms of its flexibility, initial cost, simplicity of design, ease of operation, and insensitivity to toxic substances. In addition,

*Corresponding author: Email: ngtnngoc@hcmus.edu.vn

adsorption does not result in the production of any hazardous pollutants [11]. Activated carbon is the most commonly used adsorbent in industry today, but the running costs are expensive [12]. In recent years, numerous works have been focused on the development of cheaper and more effective adsorbents. Lignocellulosic biomass has been found as a potential alternative material because these materials, including natural substances and agricultural residues, are cheap, abundant, and environmentally friendly.



Fig. 1. *Carica papaya* plant.

Carica papaya, popularly known as pawpaw, is an herbaceous fruiting plant belonging to the Caricaceae family (Fig. 1). The composition of *Carica papaya* wood (CPW) consists of crude fibre ($30.11 \pm 2.67\%$), protein ($4.96 \pm 0.68\%$), and mineral ash ($5.92 \pm 1.02\%$) [13]. CPW is a lignocellulosic biomass that mainly contains cellulose, hemicellulose, and lignin, which includes the active functional groups of carboxyl, hydroxyl, sulfhydryl, aldehydes, and ketones on the surface.

The aim of this study was to identify the biosorption potential of CPW in batch and dynamic flow systems from February to June 2018. Batch experiments were conducted to consider the influence of various operational factors such as pH, biosorbent particle size, biosorbent dosage, initial dye concentration, contact time, and salt ionic strength on the dye biosorption process. Also, the biosorbents were able to be regenerated and recyclable over many cycles. Equilibrium adsorption data were analysed by the Langmuir and Freundlich isotherm models and the constants of the isotherm equations were calculated. The continuous-flow experiments were investigated to study the effect of critical factors such as feed flow rate and biosorbent dosage. The Thomas model was used to describe the continuous-flow experimental data.

Materials and methods

Preparation of biosorbent

Carica papaya wood biomass was collected from the felled trunk of a matured papaya tree. The barks were removed, cut into small pieces and washed three times with tap water and three times with distilled water to remove dirt. After that, the biomass was dried to a constant weight at 110°C for 24 h. The dried materials were then sieved in particle sizes of 0.25, 0.5, 0.75 and 1 mm. Finally, the biosorbents were kept in airtight plastic bottles to avoid atmospheric moisture. CPW for this study was carried out without any additional pre-treatment [14].

Solutions and reagents

The stock solution of 500 mg/l of MB was prepared by dissolving 500 mg of dye in 1000 ml distilled water. All working solutions, ranging between 10 and 300 mg/l, were prepared from the stock solution by dilution with distilled water. For pH adjustment, NaOH 0.1 M and HCl 0.1 M were used.

Characterization of biosorbent

Characterization of lignocellulosic biomass has been performed by scanning electron microscopy (SEM), Fourier-transform infrared (FTIR) spectroscopy analysis, and Brunauer-Emmett-Teller (BET) analysis.

Determination of pH_{pzc} of the adsorbent

The point of zero charge (pH_{pzc}) of the biosorbent is defined as the pH at which its surface has a net neutral charge. Fifty millilitres of 0.1 M potassium nitrate was put into a series of 250 ml Erlenmeyer flasks. The solution was adjusted to an initial pH (pH_0) range between 2-10 using either 0.1 M HCl or 0.1 M NaOH. Then, 0.1 g of CPW was added to each flask and the final pH (pH_f) of the solution was measured after 24 h under an agitation speed of 150 rpm at room temperature (about 33°C). The difference between the initial pH and final pH values was calculated as $\Delta\text{pH} = \text{pH}_0 - \text{pH}_f$ and ΔpH was plotted as a function of pH_0 . The pH_0 value with a ΔpH equal to zero was called the pH_{pzc} of the biosorbent [14].

Batch biosorption studies

Batch biosorption studies were carried out to evaluate the influence of pH of the dye solution (2-12 pH), biosorbent dosage (0.1-0.8 g), particle size of the biosorbent (0.25-1 mm), and salt ionic strength (NaCl concentration 0.01-0.5 mol/l) using 50 ml of initial MB concentration (20-300 mg/l) placed in 250 ml Erlenmeyer flasks and agitated at 150 rpm for a suitable contact time (30-150 min) at room temperature. The samples were then centrifuged and the

supernatant was analysed to determine the residual MB concentration. The remaining amount of dye was determined using a UV/VIS spectrophotometer at a wavelength of 664 nm. The amount of dye adsorbed onto the biosorbent (mg dye per g biosorbent) was calculated based on Eq. (1):

$$q_e = \frac{(C_0 - C_e) \times V}{m} \quad (1)$$

where q_e is the amount of dye adsorbed at equilibrium (mg/g); C_0 and C_e are the initial and equilibrium concentrations of the MB solution (mg/l), respectively; V is the volume of solution (l); and m is the amount of biosorbent (g).

The percent removal (%) of MB was calculated using the following equation:

$$\text{Removal} = \frac{C_0 - C_e}{C_0} \times 100 \quad (2)$$

Biosorption isotherm studies

The Freundlich and Langmuir isotherms were studied by varying the dye concentration from 50-300 mg/l at a pH of 10 with an adsorbent dosage of 0.2 g, agitation speed of 150 rpm, and contact time of 30 min.

Desorption and regeneration study

Desorption of the dye from the spent adsorbent was carried out to consider its reusability. The MB-loaded CPW, after the sorption process in the optimal experimental conditions, was dried to a constant weight at 110°C for 24 h. Then, the spent adsorbent was put in contact with 50 ml of 0.1 M HCl, used as the desorbing agent, for 2 h with an agitation speed of 150 rpm. The biosorbent was thoroughly washed with distilled water several times to attain a neutral pH and then was dried in the oven. The regenerated adsorbent was reused for further adsorption studies and the sorption-desorption process was repeated for five cycles. The loss in biomass weight was determined and the biomass was then used for resorption experiments.

Continuous-flow sorption experiments

Continuous-flow sorption experiments were conducted in a 10-ml medical syringe. The biosorbent was packed into the syringe to yield the desired mass. The bottom of the syringe was covered with a layer of glass fibre in order to prevent loss of adsorbent. The MB concentration of 50 mg/l at an optimal pH of 10 flowed downward through the column at a flow rate controlled by a valve. The experiments were carried out to evaluate the influence of the feed flow rate (1, 2, 3, 4, 6 ml/min) and biosorbent mass (0.2, 0.4,

0.6, 0.8, 1.0 g). All the experiments were performed at room temperature. Operation of the continuous-flow experiments was stopped when the effluent concentration of the dye exceeded 99.5% of the initial concentration. The Thomas model was used to analyse the continuous-flow biosorption data.

Results and discussion

Characteristics of CPW

SEM analysis: SEM images (Fig. 2) were taken before adsorption at the two different magnifications (1000x and 3000x) to investigate the surface morphology of the adsorbent. SEM analysis revealed that the surface of the CPW biosorbent had a rough, uneven, and compact structure. Such a structural configuration provides attachment sites for the MB molecules.

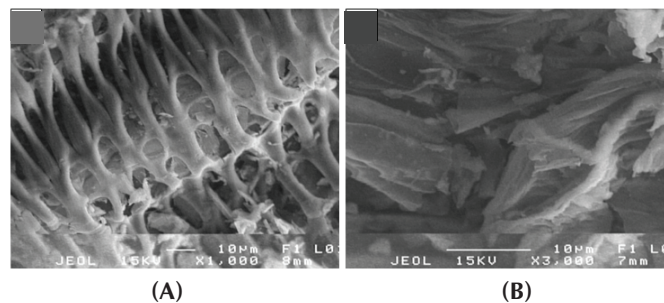


Fig. 2. SEM images of CPW at two different magnifications of 1000x (A) and 3000x (B).

FTIR analysis: FTIR analysis was used to determine the functional groups of the adsorbent and their responsibility in MB adsorption. The FTIR spectra of CPW (Fig. 3) displayed a number of absorption peaks that indicate the complex nature of the biosorbent. The broad bands at 3390 cm^{-1} represent bonded $-\text{OH}$ groups [15]. The peak at 2927.41 cm^{-1} could be assigned to the $-\text{CH}$ groups in the lignins of CPW. The peak at 1745.26 cm^{-1} corresponds to $\text{C}=\text{O}$ functional groups from the lactones and quinones. The functional group $-\text{C}=\text{O}$, from the stretching of the amid-I band in the protein peptide bond, is represented at 1610.27 cm^{-1} [16]. The COO^- peak located at 1421.28 cm^{-1} represents the carboxylate functional groups. At wave number 1317.14 cm^{-1} , a peak is observed that may be due to the $\text{C}-\text{N}$ stretching vibrations. The peak at 1238.08 cm^{-1} denotes the bending modes of functional groups $\text{O}-\text{C}-\text{H}$, $\text{C}-\text{C}-\text{H}$, and $\text{C}-\text{O}-\text{H}$. A broad band around 1052.94 cm^{-1} confirmed the presence of the functional group $\text{C}-\text{O}-\text{C}$ from the cellulose and lignin structures of CPW. The peak observed at 638.323 cm^{-1} could be assigned to the stretching of the $\text{C}-\text{Cl}$ functional groups [17, 18].

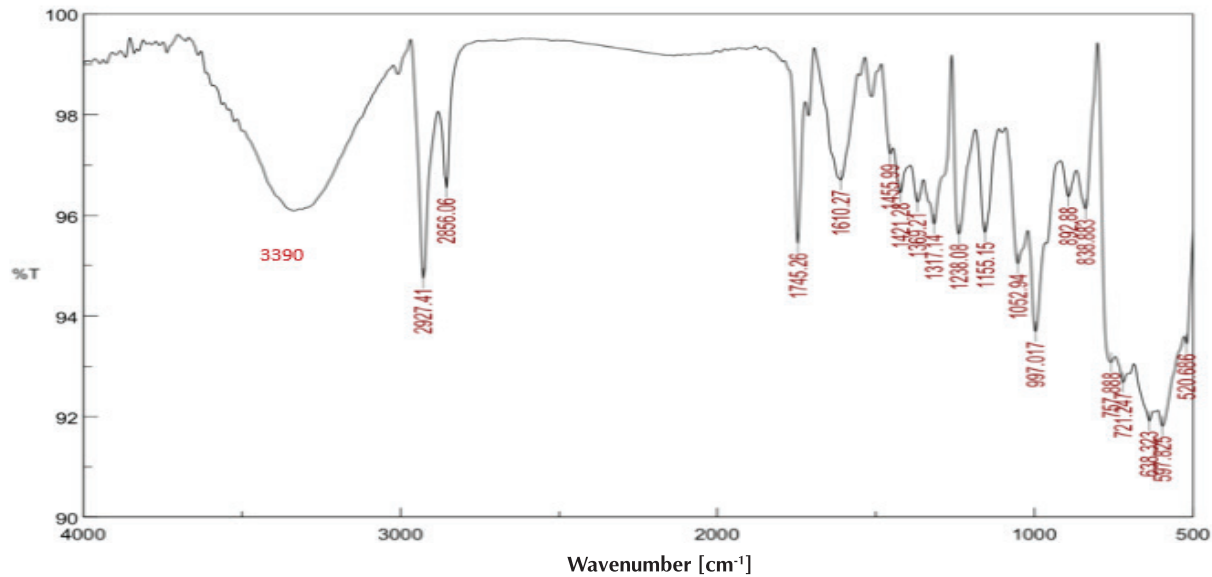


Fig. 3. FTIR spectra of CPW.

BET analysis: the BET surface area of the CPW adsorbent was found to be $0.222 \text{ m}^2/\text{g}$. This result indicates that the surface area of the CPW adsorbent was low with a total pore volume of $1.2 \text{ cm}^3/\text{g}$. These results were consistent with SEM images that revealed the CPW structure to be without voids. In addition, this examination was similar to previous literature of the BET surface area of lignocellulosic adsorbents that are of agricultural origin [19].

Batch biosorption studies

Determination of pH_{pzc} of the adsorbent: the point of zero charge (pH_{pzc}) is an important parameter that determines the linear range of pH sensitivity and indicates types of surface active centres and the adsorption abilities of surfaces [20]. A plot of ΔpH ($\Delta\text{pH} = \text{pH}_f - \text{pH}_i$) versus pH_0 for CPW is shown in Fig. 4. The pH_{pzc} of CPW was determined to be approximately 7.3. The pH_{pzc} of material showed that the CPW surface was positively charged at a solution $\text{pH} < 7.3$ and negatively charged at a solution $\text{pH} > 7.3$. This favours the biosorption of cationic dye-like MB.

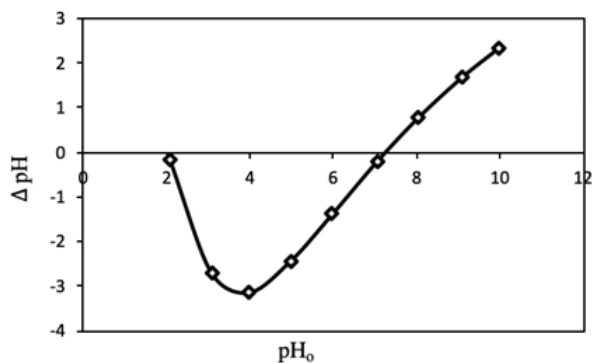


Fig. 4. pH_{pzc} of CPW.

Effect of pH: the pH plays an important role in the sorption process as it strongly affects the surface charge of the biosorbent, the degree of ionization of the adsorptive molecule, and the speciation of the biosorbate species. Fig. 5 shows the biosorption of MB by CPW over the pH range of 2 to 12. It was found that the uptake of the dye on CPW was increased with an increase in pH of the dye solution. The biosorption capacity and removal percentage of CPW for the sorption of dye was observed to increase from 7.65 to 23.38 mg/g and 30.61 to 93.51%, respectively, for an initial pH increase from 2 to 12. With a solution $\text{pH} < 6$, the dye removal by CPW showed a decrease in performance because the acidic aqueous solution produced more H^+ ions that resulted in protonation of the adsorbent surface. The lower sorption of the dye at lower pH may be because of the effects of electrostatic repulsion and competition for the biosorption sites between the excess H^+ ions and cationic groups on the dye. When the solution pH increases above pH_{pzc} , the surface of CPW becomes negatively charged due to an increase in the number of OH^- while at the same time the number of H^+ decreased. A negatively charged biosorbent

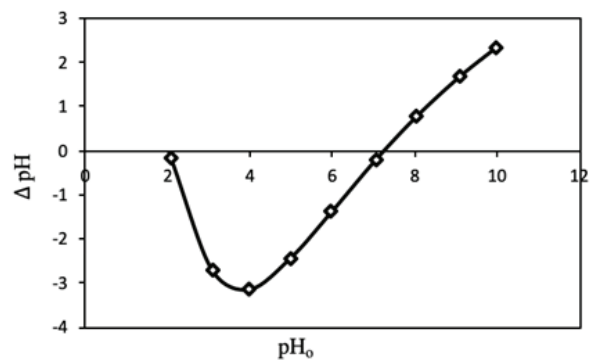


Fig. 5. Effect of initial pH on the adsorption of MB onto CPW.

surface favours the uptake of MB (or any positively charged or cationic dyes) through electrostatic attraction forces [21]. These results are in agreement with the ranges of optimal pH ($pH > pH_{pzc}$) for MB adsorption by CPW. The highest percentage of colour removal was attained at an initial pH of 10. The decrease in the adsorption of dye after a pH of 10 was insignificant. Hence, all further experiments were carried out at pH 10.

Effect of biosorbent particle size: the biosorbent particle size is a critical parameter in the sorption process because it determines the time required for the transport of sorbate within the pore to the adsorbent's active sites. The effect of the adsorbent's particle size on the uptake of MB is shown in Fig. 6. When the particle size of the adsorbent increased from 0.25 to 0.5 mm, the dye removal efficiency and biosorption capacity were almost unchanged. However, with further increase in particle size, the adsorption percentage and equilibrium sorption capacity decreased sharply. This decrease was attributed to a decrease in the surface area of the adsorbents at larger particle sizes, which provided fewer active sites to be utilized for the sorption of MB molecules [22]. Consequently, further experiments utilized at particle size of 0.5 μ m when the

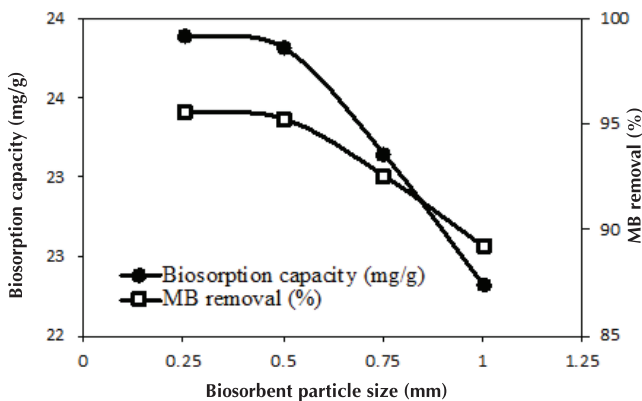


Fig. 6. Effect of biosorbent particle size on the adsorption of MB onto CPW.

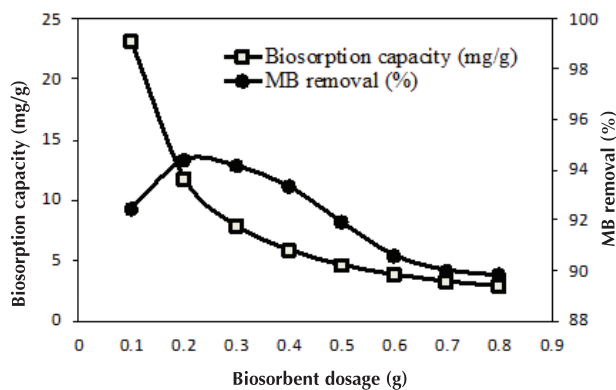


Fig. 7. Effect of biosorbent dosage on the adsorption of MB onto CPW.

effects of other experimental parameters were studied in order to achieve optimum adsorption.

Effect of biosorbent dosage: the influence of adsorbent dosage on the uptake of dye was identified by varying the amount of adsorbent from 0.1 to 0.8 g while 50 mg/l initial MB concentration and optimal pH of 10 were kept constant. The equilibrium sorption capacity and the percentage of colour removal for the different adsorbent dosages are depicted in Fig. 7. It was observed that the increase in the biosorbent dosage from 0.1 to 0.2 g resulted in an increase of removal percentage from 92.47 to 94.39%, whereas the sorption capacity of the adsorbent presented a decrease in the effect from 23.12 to 11.8 mg/g. The increase in the biosorption of MB with an increase in the adsorbent dosage was due to the higher surface area of the adsorbent and the greater number of active sites on the adsorbent. When the dose was increased above 0.2 g, the sorption of dye and the biosorption capacity decreased sharply. This can be explained by the fact that at high biosorbent dosages, the fixed number of MB molecules in solution were not enough to completely combine with all the binding sites on the biosorbent, which resulted in a reduction of the adsorption capacity per unit mass of adsorbent. Another reason for the lower percentage of colour removal is interparticle interactions such as aggregation resulting from high biosorbent concentrations. Such aggregation results in a decrease in total surface area of the adsorbent and an increase in the length of diffusion. Hence, 0.2 g of CPW was found to be optimum.

Effect of initial dye concentration: the influence of the initial concentration of dye on the equilibrium biosorption of MB by CPW was evaluated by using 0.2 g adsorbent, a solution pH of 10, and varying MB concentration from 20 to 300 mg/l. As shown in Fig. 8, the equilibrium sorption capacity increased from 4.81 to 53.08 mg/g with increased initial MB concentration. This was a result of an increase in the driving force from the concentration gradient. In addition, the binding sites of the adsorbent are surrounded by much more MB ions at high concentration of dye, which supports the accessibility for biosorption [23]. In addition, at lower MB concentrations

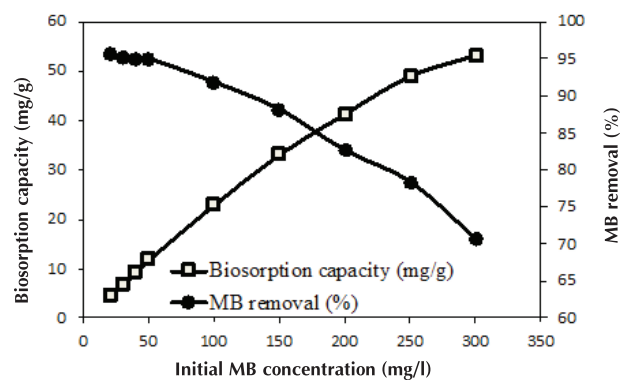


Fig. 8. Effect of initial dye concentration on the adsorption of MB onto CPW.

(20-50 mg/l), all the dye molecules are able to interact with the large number of binding sites, hence, a higher percentage of dye removal. An increase in the MB concentration (>50 mg/l) occurred from the decrease in the biosorption of dye due to the saturation of active sites [24]. Fig. 8 showed that a high removal efficiency was attained at an initial MB concentration of 50 mg/l.

Effect of contact time: the results of changing contact time is represented in Fig. 9. It can be seen that the uptake of dyes was rapid in the initial adsorption period (in the first 60 min). The fast biosorption rate at this initial stage indicates the instantaneous adsorption or external surface adsorption of MB onto CPW [25]. In addition, the higher uptake rate in the initial period may be because of the greater number of binding sites available on the biosorbent and because of the strong attractive forces between the biosorbent and dye molecules. At longer contact times (after 60 min) the rate of biosorption decreased and tended to slow down. After 90 min, the curve plateaued, which showed no considerable adsorption of dye. It can be explained that the number of active sites available for sorption decreased. However, the percentage of MB removal increased slightly from 95.22 to 97.25% for a contact time increase from 30 to 60 min. Therefore, the optimal time for the sorption of the dye was 30 min with 95.22% MB removal efficiency.

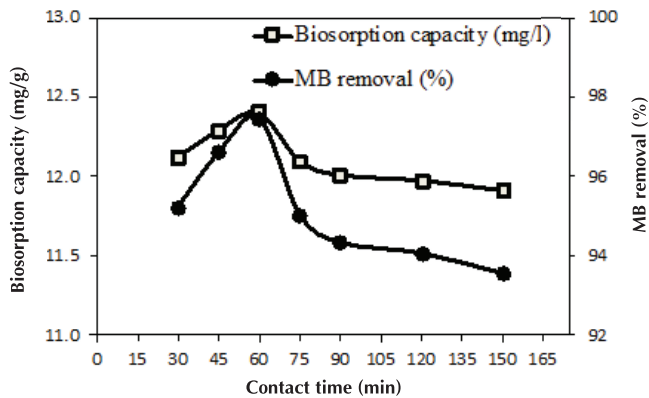


Fig. 9. Effect of contact time on the adsorption of MB onto CPW.

Effect of salt ionic strength on the dyes biosorption: textile industries consume large amounts of salt during the dyeing process, so the influence of salts on biosorption was evaluated in this study. The variation of the salt concentration depends on the source and type of the industrial effluents [26]. Sodium chloride (NaCl) is known as a stimulator in the dyeing process, which can affect electrostatic interactions of the dye molecules. To examine how salt concentration affects the biosorption of MB onto CPW, the experiment was carried out with varying NaCl concentrations from 0.01-0.5 M in the dye solution. The results are illustrated in Fig. 10. It was found that the sorption

of dye decreased from 85.70 to 41.72% for the increase in the NaCl concentration from 0.01 to 0.5 M. The uptake of dye was significantly affected by the presence of high NaCl concentrations. The decrease in the percentage of dye removal was due to the competition between MB and Na⁺ cation for the adsorption of active sites on the biosorbent. Thus, the increase in ionic strength led to a decrease in the adsorption potential of CPW for MB removal. Previous literature also reported that MB adsorption declined considerably with the presence of NaCl in aqueous solutions [27].

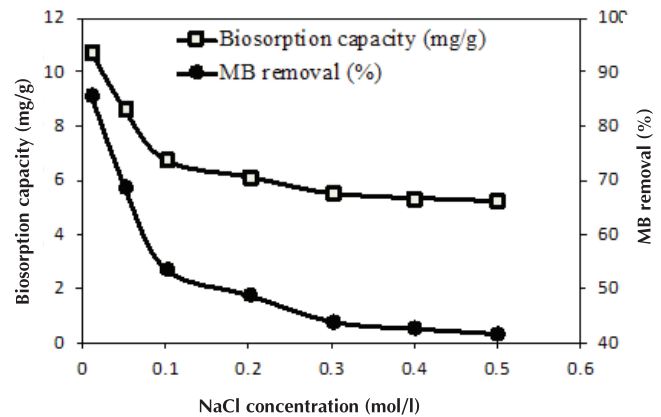


Fig. 10. Effect of NaCl concentrations on the adsorption of MB onto CPW.

Adsorption isotherm: analysis of the adsorption isotherm is of fundamental importance to the evaluation of the interaction of adsorbate molecules with the adsorbent surface. Isotherm studies also calculate the maximum biosorption capacity and equilibrium constants, which express the affinity of the biosorbent. The Freundlich and Langmuir isotherm models were applied to describe the equilibrium biosorption data (Fig. 11).

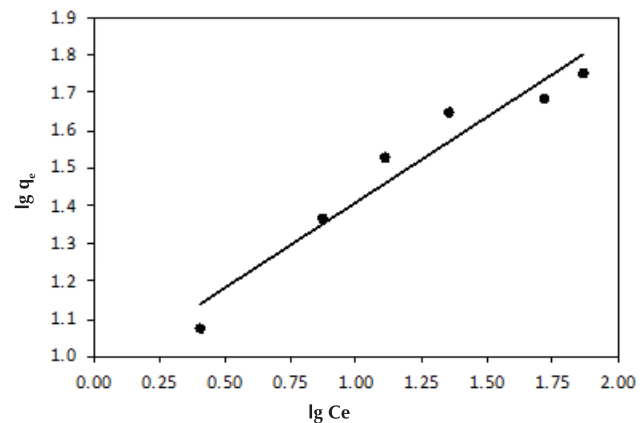


Fig. 11. Freundlich isotherm plots for MB biosorption onto CPW.

The Freundlich model: the Freundlich model is an empirical equation that can be applied to multilayer sorption with a non-uniform distribution of sorption heat and affinity over the heterogeneous surface. The Freundlich equation is given as:

$$q_e = K_F C_e^{1/n} \tag{3}$$

where K_F is Freundlich constant, which is an indicator for adsorption capacity, and $1/n$ is the adsorption intensity. A value of $0 < 1/n < 1$ shows adsorption surface homogeneity. As the value gets closer to 0, the adsorption process is heterogeneous [28]. A value for $1/n < 1$ shows a normal Langmuir isotherm while $1/n > 1$ indicates cooperative adsorption [29]. The linear form of the Freundlich equation is given as:

$$\lg q_e = \lg K_F + \left(\frac{1}{n}\right) \lg C_e \tag{4}$$

The values of K_F and n are listed in Table 2. Both the values are calculated from the intercept and slope of the plot of $\lg q_e$ versus $\lg C_e$. The value of $1/n$ is 0.45, from a range between 0 and 1, which showed that the dye uptake by CPW is favourable for sorption. Moreover, the K_F constant of 9.1 l/g indicated a high dye uptake capacity.

The Langmuir model: the Langmuir adsorption model assumes that the adsorbent surface is homogeneous in character and the formation of a monolayer takes place on the surface of the adsorbent. The Langmuir model is given by the following equation:

$$q_e = \frac{Q_0 K_L C_e}{1 + K_L C_e} \tag{5}$$

where Q_0 is the maximum amount of the adsorbed dye per unit mass of adsorbent to form a complete monolayer on the surface bound at concentration C_e (mg/g) and K_L (l/mg) is the Langmuir constant related to the affinity of the binding sites. The Langmuir model can be represented in linear form as:

$$\frac{C_e}{q_e} = \frac{1}{Q_0 K_L} + \frac{C_e}{Q_0} \tag{6}$$

The essential characteristics of the Langmuir isotherm can be expressed in terms of the separation factor R_L , which is a dimensionless constant in Eq. (7):

$$R_L = \frac{1}{(1 + K_L C_0)} \tag{7}$$

A favourable biosorption takes place if $0 < R_L < 1$, whereas $R_L > 1$ shows unfavourable biosorption, $R_L = 1$ shows linear biosorption conditions, and $R_L = 0$ shows irreversible biosorption conditions [30].

The linear plot of Langmuir isotherm and the plot of the separation factor as a function of initial concentration of MB are shown in Figs. 12 and 13, respectively. The parameters obtained from the Langmuir and Freundlich isotherm plots

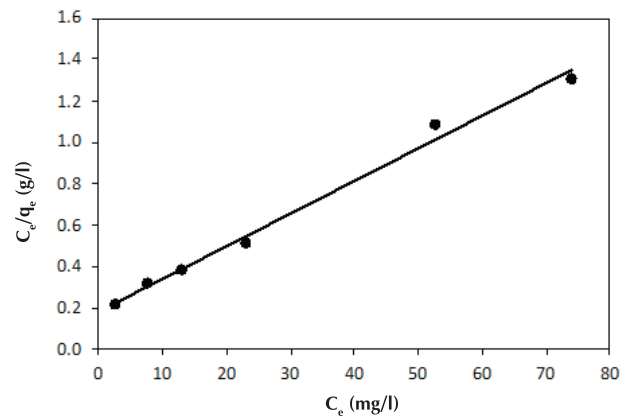


Fig. 12. Langmuir isotherm plots for MB biosorption onto CPW.

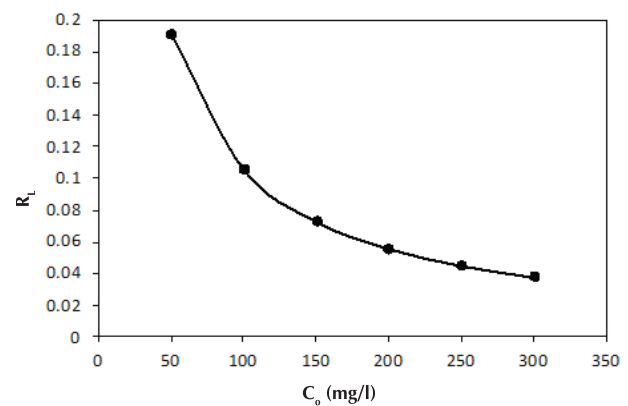


Fig. 13. Effect of initial dye concentration on separation factor.

are listed in Table 2. Analysis of the R values suggests that the Langmuir isotherm model provided a better fitting compared to the Freundlich isotherm models. This implies monolayer coverage of MB molecules onto the CPW surface. This suggestion is consistent with the results of FTIR and SEM shown in Figs. 2 and 3. In essence, the CPW biosorbent has a compact structure without voids, so the adsorption process occurs mainly on the surface of CPW. MB molecules were kept by chemical functional groups such as $-OH$, $C=O$, and COO^- inside the CPW structure as seen in the FTIR spectrum of Fig. 3. The values of the separation factor, R_L , are between 0 and 1 indicating that the dye uptake by CPW are favourable.

Table 2. Biosorption isotherm constants for the biosorption of MB onto CPW at room temperature.

Langmuir constants			Freundlich constants		
Q_0 (mg/g)	K_L (l/mg)	R^2	K_F (l/g)	$1/n$	R^2
63.29	0.085	0.9914	9.1	0.45	0.936

Table 3 summarizes the maximum MB sorption capacity of various low-cost sorbent materials. It can be seen that CPW has high biosorption capacity of MB compare to many of the other reported biosorbents. Differences in the sorption of dye can be explained by the different characteristics of adsorbent materials such as structure, functional groups, and surface area. CPW is an abundant and low-cost material, which makes it a potential biosorbent for the removal of MB from aqueous solutions.

Table 3. Comparison of MB biosorption capacity of CPW with others reported low-cost sorbents.

Adsorbent	Maximum sorption capacity (mg/g)	References
Rice bran	54.99	[31]
Wheat bran	54.79	[31]
Unmodified biomass of baker's yeast	51.5	[11]
Parthenium hysterophorus unwanted weed	39.68	[32]
Coir pith carbon	5.87	[33]
Coconut coir dust	19.61	[34]
Tartaric acid modified bagasse	69.93	[30]
Cereal chaff	20.30	[35]
<i>Carica papaya</i> wood	32.25	[14]
<i>Carica papaya</i> wood	63.29	This study

Desorption and regeneration study: the adsorption capacity of the regenerated biosorbent was carried out over five repeated cycles using 50 ml HCl 0.1 M as the desorbing eluent. The desorption and resorption of MB on the CPW biosorbent is shown in Table 4. The eluent was able to maintain an elution efficiency of more than 90% over the first three cycles, then the efficiency decreased slightly for the next two cycles. However, the final results of the regeneration of MB maintained more than 80% of the sorption of the dye over 5 cycles. Furthermore, a significant biosorbent weight loss was observed during the 4th and 5th regeneration cycles. It is known that the slightly acidic nature of the desorbing agent and the damage in physical-chemical structure of the biosorbent have caused biomass weight loss in subsequent cycles [36]. In addition, the sorption decrease in subsequent cycles may be due to the blockage of the active sites of the biosorbent. The desorption and resorption experiments showed that the CPW has great potential for recycling performance.

Table 4. Desorption and resorption of MB on CPW biosorbent.

Cycle no.	MB removal (%)	Weight loss (%)
1	94.68	7.5
2	94.09	15
3	93.27	26
4	88.48	41.25
5	85.25	48.75

Continuous-flow sorption study

Effect of flow rate: the flow rate is a significant characteristic of the sorption process in the continuous treatment of wastewater on an industrial scale [37]. In this study, the influence of flow rate on MB removal by CPW was performed by varying the flow rate in the range of 1-5 ml/min, maintaining an initial MB concentration of 50 mg/l, solution pH of 10, and adsorbent dose of 0.2 g optimized in batch studies. The effect of flow rate on the percentage of dye removal with the above operating conditions is depicted in Fig. 14. It was observed that the uptake of dye was higher at a lower flow rate. At a lower flow rate, there is an increased contact time with the MB solution and therefore the dye had more time to bind with the active sites in the adsorbent [38]. The MB molecules also have more time to diffuse into the pores of the biosorbent through intraparticle diffusion. As the flow rate is increased, the residence time of the MB solution in the column decreases. Then, the residence time of the solute in the column is not large enough for the dye molecules to diffuse into the pores of the adsorbent and capture the active sites on the biosorbent surface leaving the column before equilibrium occurs [39]. Considering the percentage of dye removal and economic efficiency, further experiments were carried out at a flow rate of 2 ml/min.

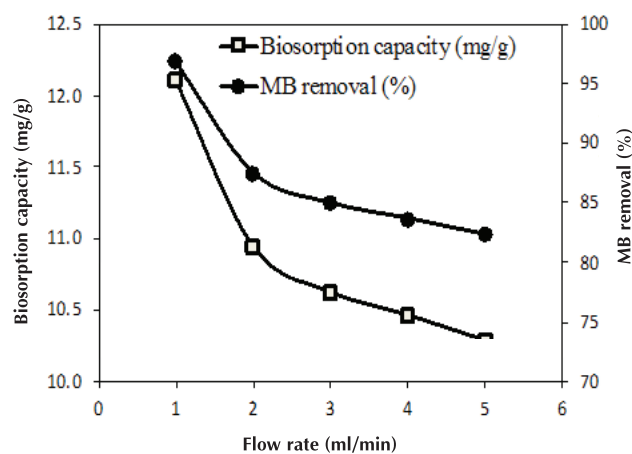


Fig. 14. Effect of flow rate on MB removal in continuous-flow biosorption study.

Effect of adsorbent dosage: the experiments were conducted at adsorbent dosages of 0.2 to 1.0 g at a constant flow rate of 2 ml/min and feed concentration of 50 mg/l. The effect of the biosorbent dosage on MB removal in the continuous-flow experiments is represented in Fig. 15. As the adsorbent dose is increased by a factor of 2 from 0.2 to 0.4 g, the MB removal efficiency sharply increased from 87.55 to 95.54%. Then, the removal efficiency showed no significant change as the biosorbent dosage was increased, which demonstrated that 0.4 g should be chosen as the optimal biosorbent dosage for the remaining experiments.

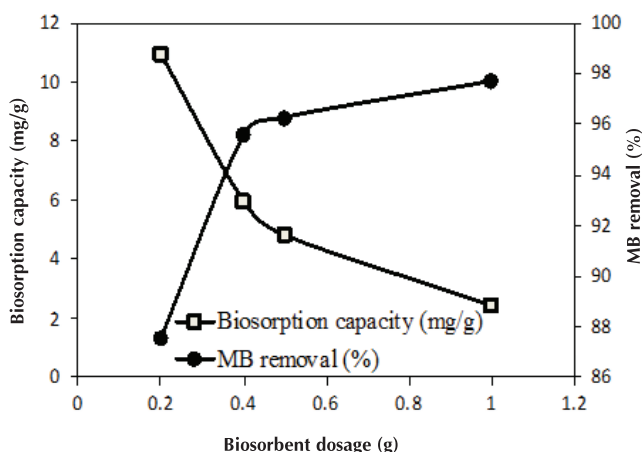


Fig. 15. Effect of biosorbent dosage on MB removal in continuous-flow biosorption study.

Application of Thomas model: the Thomas model is one of the most common and widely used models to estimate the adsorption in column performance theory. The model is based on the assumption that the process follows second-order reversible reaction kinetics and the Langmuir isotherm [40]. The linearized form of the Thomas model can be expressed as follows:

$$\ln\left(\frac{C_0}{C_t} - 1\right) = \frac{k_{Th}q_0w}{Q} - k_{Th}C_0t$$

where k_{Th} (ml/min/mg) is the Thomas rate constant; q_0 (mg/g) is the equilibrium MB uptake per g of the adsorbent; C_0 (mg/l) is the influent dye concentration; C_t (mg/l) is the effluent dye concentration at time t ; w (g) is the mass of adsorbent in the column, and Q (ml/min) is the flow rate. A linear plot of $\ln(C_0/C_t - 1)$ versus time (t) is depicted in Fig. 16. The values of k_{Th} and q_0 are determined from the intercept and slope of the plot. The values of k_{Th} and q_0 , calculated from Eq. (8), were 2.6×10^{-4} (ml/mg/min) and 80.47 mg/g, respectively. The relatively high R^2 ($R^2=0.9747$) value suggests that the Thomas model was suitable to describe the column data of MB by CPW. The calculated q_e values ($q_e=81.82$ mg/l) show good agreement with the experimental q_e values ($q_e=79.4$ mg/l), which further confirms the suitability of the Thomas model for column design and analysis.

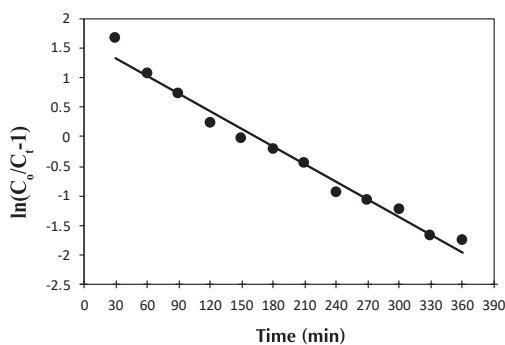


Fig. 16. Thomas model plots for the biosorption of MB onto CPW.

Conclusions

The present study on the adsorption of MB using CPW suggested the following conclusions:

- The results showed that equilibrium was attained within 30 min and the maximum adsorption capacity of MB onto CPW was obtained after contact with 0.2 g of biosorbent, a biosorbent particle size of 0.5 mm, initial solution pH of 10.0, and dye concentration of 50 mg/l. The experimental data showed an excellent fit to the Langmuir isotherm equation, which provided a 63.29 mg/g monolayer biosorption capacity of MB onto CPW.

- Continuous-flow biosorption experiments indicated that the adsorbent dosage and flow rate affected the biosorption characteristics of CPW with a biosorbent dosage of 0.4 g and a flow rate of 2 ml/min resulting in optimal MB removal. The Thomas model adequately described the biosorption of MB onto CPW by a continuous-flow mode.

- The biomass from *Carica papaya* wood has been shown to be highly effective in removing MB from an aqueous solution. The study revealed that this new biosorbent is a very prospective adsorbent for the removal MB from industrial wastewater.

COMPETING INTERESTS

The authors declare that there is no conflict of interest regarding the publication of this article.

REFERENCES

- [1] S. Manna, D. Roy, P. Saha, D. Gopakumar, S. Thomas (2017), "Rapid methylene blue adsorption using modified lignocellulosic materials", *Safety and Environment Protection*, **107**, pp.346-356.
- [2] J. Song, W. Zou, Y. Bian, F. Su, R. Han (2011), "Adsorption characteristics of methylene blue by peanut husk in batch and column modes", *Desalination*, **265**, pp.119-125.
- [3] V. Vimonses, S. Lei, B. Jin, C.W.K. Chow, C. Saint (2009), "Kinetic study and equilibrium isotherm analysis of Congo Red adsorption by clay materials", *Chemical Engineering Journal*, **148**, pp.354-364.
- [4] K. Kadirvelu, M. Kavipriya, C. Karthika, M. Radhika, N. Vennilamani, S. Pattabhi (2003), "Utilization of various agricultural wastes for activated carbon preparation and application for the removal of dyes and metal ions from aqueous solutions", *Bioresource Technology*, **87**, pp.129-132.
- [5] A.R. Dincer, Y. Günes, N. Karakaya, E. Günes (2007), "Comparison of activated carbon and bottom ash for removal of reactive dye from aqueous solution", *Bioresource Technology*, **98**, pp.834-839.
- [6] D. Shen, J. Fan, W. Zhou, B. Gao, Q. Yue, Q. Kang (2009), "Adsorption kinetic sand isotherm of anionic dyes onto organo-bentonite from single and multisolute systems", *Journal of Hazardous Materials*, **172**, pp.99-107.
- [7] M.T. Uddin, M.A. Islam, S. Mahmud, M. Rukanuzzaman (2009), "Adsorptive removal of methylene blue by tea waste", *Journal of Hazardous Materials*, **164**, pp.53-60.
- [8] A.K. Jain, V.K. Gupta, A. Bhatnagar, Suhas (2003), "Utilization of industrial waste products as adsorbents for the removal of dyes", *Journal of Hazardous Materials*, **B101**, pp.31-42.

- [9] Y.S. Ho, G. McKay (2003), "Sorption of dyes and copper ions onto biosorbents", *Process Biochemistry*, **38**, pp.1047-1061.
- [10] F. Derbyshire, M. Jagtoyen, R. Andrews, A. Rao, I. Martin-Gullon, E. Grulke (2001), "Carbon materials in environmental applications", *Chemistry and Physics of Carbon*, **27**, pp.1-66.
- [11] M. Rafatullah, O. Sulaiman, R. Hashim, A. Ahmad (2010), "Adsorption of methylene blue on low-cost adsorbents: a review", *Journal of Hazardous Materials*, **177**, pp.70-80.
- [12] S. Wang, Z.H. Zhu, A. Coomes, F. Haghseresht, G.Q. Lu (2005), "The physical and surface chemical characteristics of activated carbons and the adsorption of methylene blue from wastewater", *Journal of Colloid and Interface Science*, **284**, pp.440-446.
- [13] S. Basha, Z.V.P. Murthy, B. Jha (2009), "Sorption of Hg(II) onto *Carica papaya*: experimental studies and design of batch sorber", *Chemical Engineering Journal*, **147**, pp.226-234.
- [14] S. Rangabhashiyam, S. Lata, P. Balasubramanian (2018), "Biosorption characteristics of methylene blue and malachite green from simulated wastewater onto *Carica papaya* wood biosorbent", *Surfaces and Interfaces*, **10**, pp.197-215.
- [15] S. Rangabhashiyam, N. Selvaraju (2015), "Adsorptive remediation of hexavalent chromium from synthetic wastewater by a natural and ZnCl₂ activated *Sterculia guttata* shell", *Journal of Molecular Liquids*, **207**, pp.39-49.
- [16] T. Akar, B. Anilan, A. Gorgulu, S.T. Akar (2009), "Assessment of cationic dye biosorption characteristics of untreated and non-conventional biomass: *Pyracantha coccinea* berries", *Journal of Hazardous Materials*, **168**, pp.1302-1309.
- [17] R. Han, L. Zhang, C. Song, M. Zhang, H. Zhu, L. Zhang (2010), "Characterization of modified wheat straw, kinetic and equilibrium study about copper ion and methylene blue adsorption in batch mode", *Carbohydrate Polymers*, **79**, pp.1140-1149.
- [18] M.C.S. Reddy, L. Sivaramakrishna, A.V. Reddy (2012), "The use of an agricultural waste material, *Jujuba* seeds for the removal of anionic dye (congo red) from aqueous medium", *Journal of Hazardous Materials*, **203-204**, pp.118-127.
- [19] E.D. Asuquo, A.D. Martin, P. Nzerem (2018), "Evaluation of Cd(II) ion removal from aqueous solution by a low-cost adsorbent prepared from white yam (*Dioscorea rotundata*) waste using batch sorption", *Chemical Engineering*, **2**, DOI: 10.3390/chemengineering2030035.
- [20] A.A. Poghosian (1997), "Determination of the pH_{pzc} of insulators surface from capacitance - voltage characteristics of MIS and EIS structures", *Sensors and Actuator B: Chemical*, **44**, pp.551-553.
- [21] P.S. Kumar, S. Ramalingam, C. Senthamarai, M. Niranjanaa, P. Vijayalakshmi, S. Sivanesan (2010), "Adsorption of dye from aqueous solution by cashew nut shell: studies on equilibrium isotherm, kinetics and thermodynamics of interactions", *Desalination*, **261**, pp.52-60.
- [22] K.K. Wong, C.K. Lee, K.S. Low, M.J. Haron (2003), "Removal of Cu and Pb by tartaric acid modified rice husk from aqueous solutions", *Chemosphere*, **50**, pp.23-28.
- [23] R. Han, J. Zhang, P. Han, Y. Wang, Z. Zhao, M. Tang (2009), "Study of equilibrium, kinetic and thermodynamic parameters about methylene blue adsorption onto natural zeolite", *Chemical Engineering Journal*, **145**, pp.496-504.
- [24] S. Chowdhury, R. Mishra, P. Saha, P. Kushwaha (2011), "Adsorption thermodynamics, kinetics and isosteric heat of adsorption of malachite green onto chemically modified rice husk", *Desalination*, **265**, pp.159-168.
- [25] P. Saha, S. Chowdhury, S. Gupta, I. Kumar (2010), "Insight into adsorption equilibrium, kinetics and thermodynamics of malachite green onto clayey soil of Indian origin", *Chemical Engineering Journal*, **165**, pp.874-882.
- [26] D. Mitrogiannis, G. Markou, A. Celekli, H. Bozkurt (2015), "Biosorption of methylene blue onto *Arthrospira platensis* biomass: kinetic, equilibrium and thermodynamic studies", *Journal of Environmental Chemical Engineering*, **3**, pp.670-680.
- [27] G. Jian-Zhong, L. Bing, L. Li, L. Kangle (2014), "Removal of methylene blue from aqueous solutions by chemically modified bamboo", *Chemosphere*, **111**, pp.225-231.
- [28] B.H. Hameed, D.K. Mahmoud, A.L. Ahmad (2008), "Sorption equilibrium and kinetics of basic dye from aqueous solution using banana stalk waste", *Journal of Hazardous Materials*, **158**, pp.499-506.
- [29] K. Fytianos, E. Voudrias, E. Kokkalis (2000), "Sorption desorption behavior of 2,4-dichlorophenol by marine sediments", *Chemosphere*, **40**, pp.3-6.
- [30] L.W. Low, T.T. Teng, M. Rafatullah, N. Morad, B. Azahari (2013), "Adsorption studies of Methylene blue and Malachite green from aqueous solutions by pretreated lignocellulosic materials", *Separation Science and Technology*, **48**, pp.1688-1698.
- [31] X.S. Wang, Y. Zhou, Y. Jiang, C. Sun (2008), "The removal of basic dyes from aqueous solutions using agricultural by-products", *Journal of Hazardous Materials*, **157**, pp.374-385.
- [32] H. Lata, V.V. Garg, R.K. Gupta (2007), "Removal of a basic dye from aqueous solution by adsorption using *Parthenium hysterophorus*: an agricultural waste", *Dyes and Pigments*, **74**, pp.653-658.
- [33] D. Kavitha, C. Namasivayam (2007), "Experimental and kinetic studies on methylene blue adsorption by coir pith carbon", *Bioresource Technology*, **98**, pp.14-21.
- [34] K.G. Bhattacharyya, A. Sharma (2005), "Kinetics and thermodynamics of methylene blue adsorption on neem (*azadirachta indica*) leaf powder", *Dyes and Pigments*, **65**, pp.51-59.
- [35] H. Runping, W. Yuanfeng, H. Pan, S. Jie, Y. Jian, L. Yongsen (2006), "Removal of methylene blue from aqueous solution by chaff in batch mode", *Journal of Hazardous Materials*, **137**, pp.550-557.
- [36] K. Vijayaraghavan, J. Jegan, K. Palanivelu, M. Velan (2005), "Biosorption of Cobalt (II) and Nickel (II) by seaweeds: batch and column studies", *Separation and Purification Technology*, **44**, pp.53-59.
- [37] P.D. Saha, S. Chowdhury, M. Mondal, K. Sinha (2012), "Biosorption of direct red 28 (congo red) from aqueous solutions by eggshells: batch and column studies", *Separation Science and Technology*, **47**, pp.112-113.
- [38] A.A. Ahmad, B.H. Hameed (2020), "Fixed-bed adsorption of reactive azo dye onto granular activated carbon prepared from waste", *Journal of Hazardous Materials*, **175**, pp.298-303.
- [39] V. Vinodini, N. Das (2010), "Packed bed column studies on Cr(VI) removal from tannery wastewater by neem sawdust", *Desalination*, **264**, pp.9-14.
- [40] P.D. Saha, S. Chakraborty, S. Chowdhury (2012), "Batch and continuous (fixed-bed column) biosorption of crystal violet by *Artocarpus heterophyllus* (jackfruit) leaf powder", *Colloids and Surfaces B: Biointerfaces*, **92**, pp.262-270.